

## **STRESS BEHAVIOUR OF 3D PRINTED PLATE WITH HOLE**

Kuntjoro, W., Abdul Jalil\*, A.M.H., Ahmad Redzuan, A.N, Mohd Nasir, R.E.

Flight Technology and Test Center (FTTC), College of Engineering, MARA University of Technology (UiTM), 40450 Shah Alam, Selangor Darul Ehsan, Malaysia.

\* Corresponding Author: [abdulmalikhussein@gmail.com](mailto:abdulmalikhussein@gmail.com) TEL: (+60)-192386966

---

**Abstract:** This study calculates the stress concentration factor of flat and curved PLA plate structures and studies the stress features surrounding holes of the plate structure. It is essential to understand the stress behaviour of 3D-printed PLA plates around the hole. Flat and curved plates with holes of 40 mm, 20 mm, and 10 mm in diameter were investigated. With a 2.5 N/mm<sup>2</sup> applied load to the plate, such models were put through finite element analysis and simulations using ANSYS to investigate the maximum stress in the longitudinal direction. The result was then compared to the theoretical result. The results show that for the curve radius of 100 mm, decreasing the hole diameter of 0.04, 0.02 and 0.01 m increases the stress concentration factor of 2.18, 2.41 and 2.68 respectively. The stress versus diameter graph for elements with dimensions of 5 mm, 4 mm, and 2 mm compares the maximum stress between analysis methods and finite element analysis. The results show that for the curve radius of 100 mm hole diameter of 40, 20 and 10 mm with element size of 2 mm, will produce the decreasing maximum stress of 10.7063, 8.0046 and 7.5529 MPa. The Stress Concentration Factor ( $K_t$ ) vs. Plate Diameter graph indicates that the stress concentration factor increases with decreasing diameter. The maximum stress is demonstrated to be decreasing as the hole gets smaller.

Keywords: 3D Printing; Plate with Hole; PLA; Finite Element Analysis; Stress Concentration Factor.

---

## 1. Introduction

In engineering, plate structures with holes are commonly utilized in aerospace structures (Kim & Park, 2020; Mo et al., 2019). Wing structures have lots of panels with holes (Pukale & Amarnadha Reddy, 2014). **Figure 1** below displays a schematic diagram of aircraft structures with holes.

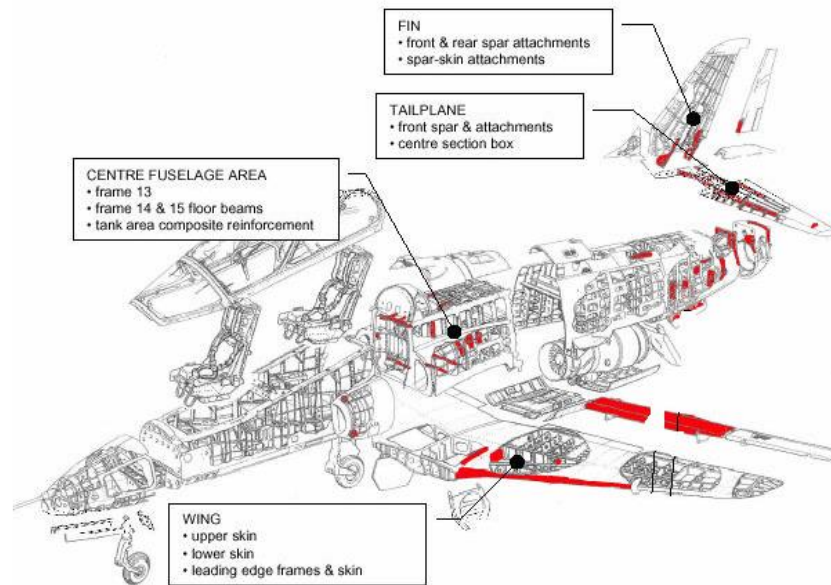


**Figure 1.** Example of Aircraft Structures with Holes (Ansell, 2015)

3D printing was previously used to create prototypes, not structural engineering components, for the aircraft industry (Guduru & Srinivasu, 2020). Expanding the usability of 3D printing for getting sturdy engineering parts for those applications is becoming an important goal of industrial use (Guduru & Srinivasu, 2020; Ngo et al., 2018). 3D printing is a technology that allows us to translate complex geometry into a physical model (Raj et al., 2018). However, there are significant drawbacks to this manufacturing technique, including the necessity for support material and a subpar surface polish (Lalehpour & Barari, 2016). Polylactic Acid (PLA) is commonly used for applications in the 3D printing industry. PLA is not commonly used in the aircraft industry. PLA processing is more accessible and safer with a smoother and shinier surface. Structural design and optimization can be done to improve performance (Ertane et al., 2018). PLA also has a relatively high level of strength, which is essential in 3D printing modern

components (Raj et al., 2018). Hole is important in aircraft structures for inspection purposes, to reduce weight or even for having windows.

The Finite Element Analysis (FEA) approach is a standard simulation technique. FEA divides a massive configuration with many physical difficulties and mathematical discontinuities into smaller, easier-to-manage pieces (Kolodziej, 2019). To design such plates with holes, precise knowledge in deflection, loads, and stress concentration factor is required (Jain & Mittal, 2008). A stress concentration factor impacts structural design more (Zappino et al., 2020). Finite element analysis can be used to compare the analytical and experimental results of stress distribution of plates with different holes (Pawar et al., 2016). For any finite element analysis, mesh refinement is vital in generating reliable solutions in finite element analysis (Ding, 2006; Mekalke et al., 2009). The finite element method has also been applied to the modelling and analysis of 3D printed box structures to simulate a simple wing box type structure (Kuntjoro et al., 2021).

For this study, the problem to address here is the stress features around the holes of PLA generated by 3D printing and the stress concentration factor of the holes. The analysis was carried out with the help of ANSYS<sup>®</sup>, a finite element analysis software, and the results were validated using an analytical method. The popular general-purpose finite element analysis program ANSYS<sup>®</sup>, which was first introduced in 1971, can be used to resolve static and dynamic structural, fluid flow, heat transport, and electromagnetic calculations (Thompson & Thompson, 2017). All simulations are still run through a coding language called ANSYS Parametric Design Language (APDL), despite recent versions of ANSYS<sup>®</sup> having an easy graphical user interface (GUI) called Workbench<sup>™</sup>. By writing unique scripts that execute at predetermined intervals, Workbench<sup>™</sup> allows users to include custom APDL code into a standard finite element analysis.

## **2. Finite Element Modelling and Analysis**

### **2.1. Important Parameters of the Model**

In ANSYS, a flat plate was modelled as a rectangular section with dimensions of 200 mm in length, 80 mm in width, and 1 mm thick. A curve plate has a length of 200 mm, a width of 80.3 mm, 83.8 mm, or 88 mm (depending on the curve radius), and the thickness of 1 mm was also simulated on ANSYS. The holes on the flat and curved plates are 40 mm, 20 mm, and 10 mm in diameter, as described in **Table 1**. The left end is fixed, and the right is subjected to a 2.5

N/mm<sup>2</sup> load. The value of 2.5 N/mm<sup>2</sup> is regarded as appropriate for this investigation as this is not going to break the structure. It is modelled using PLA material, with varied element sizes of 5 mm, 4 mm, and 2 mm. This size of shell element is appropriate for the size and thickness of this panel. The following are the material properties, as listed in **Table 2** below (Agrawal et al., 2021):

**Table 1.** Geometries of Plates

Type of Plate	Length (mm)	Thickness (mm)	Width (mm)	Curve Radius (mm)	Hole Diameter (mm)
Flat	200	1	80	N/A	40
					20
					10
Curve	200	1	80.3	100	40
					20
					10
			83.8	80	40
					20
					10
			88	60	40
					20
					10

**Table 2.** Material Properties (Agrawal et al., 2021)

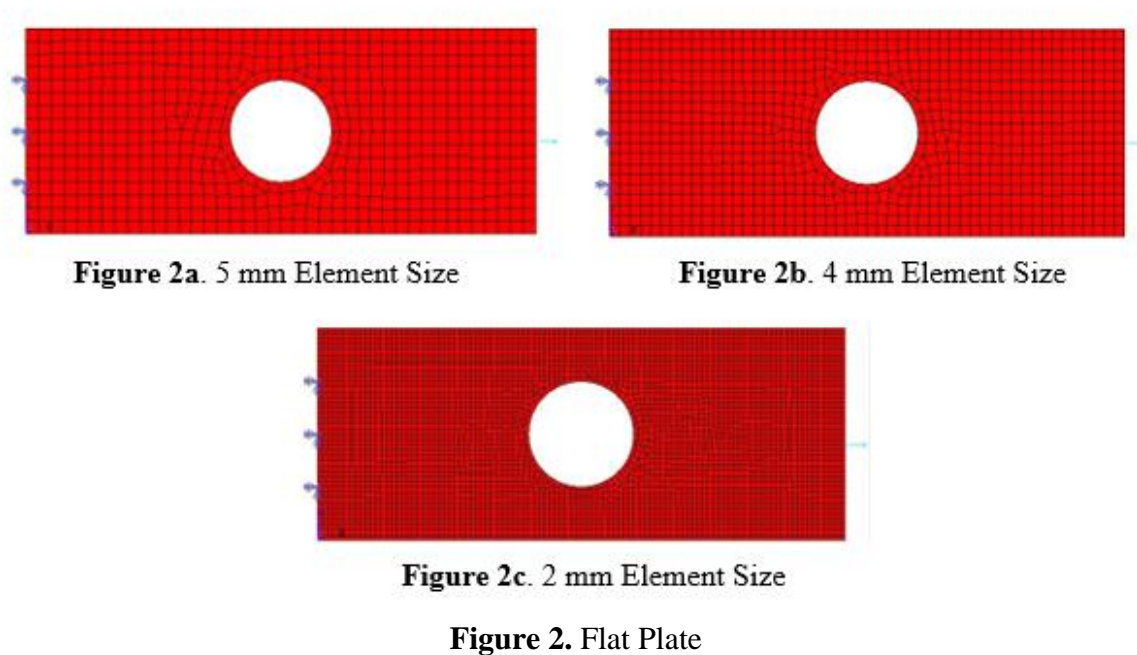
Material	Young's Modulus (MPa), $E_x$	Young's Modulus (MPa), $E_y=E_z$	Poisson's Ratio	Shear Modulus (MPa), $G_{xy}=G_{yz}$	Shear Modulus (MPa), $G_{xz}$
PLA	1510	1430	0.33	560	530

## 2.2 Finite Element Model using ANSYS

Finite element modelling was done using ANSYS<sup>®</sup>. Holes in the sizes of 40 mm, 20 mm, and 10 mm in diameter were designed for both flat and curved plates. 5 mm, 4 mm and 2 mm element size were used in this study.

### 2.2.1 Flat Plate

The flat plates were modelled as described in **Table 1**. Each flat plate was analysed using elements measuring 5 mm, 4 mm, and 2 mm in size. The material used is tabulated in **Table 2**. The applied load was  $2.5 \text{ N/mm}^2$  at the right end of the plate, whereas the left end was fixed. The maximum stress in the longitudinal direction was measured. The diagram below in **Figure 2** depicts the force and fixed support for a flat plate with a hole diameter of 40 mm and element sizes of 5 mm, 4 mm, and 2 mm.



### 2.2.2 Curved Plate

Each curved plate was analysed using 5 mm, 4 mm, and 2 mm element sizes. The load and boundary conditions were applied the same way as the flat plate. The maximum stresses in the longitudinal direction were calculated. The force and fixed support are described in **Figure 3** below with a 5 mm element size.

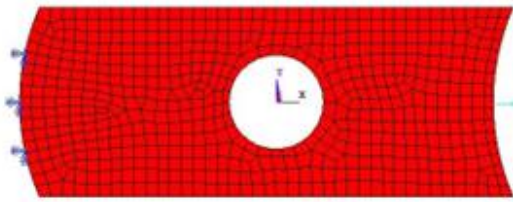


**Figure 3a.** 100 mm Curved Radius

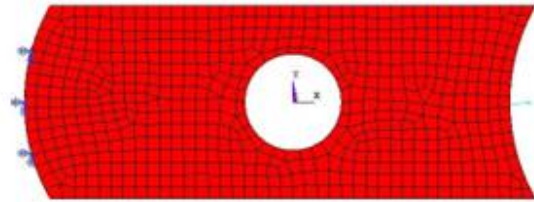


**Figure 3b.** 80 mm Curved Radius

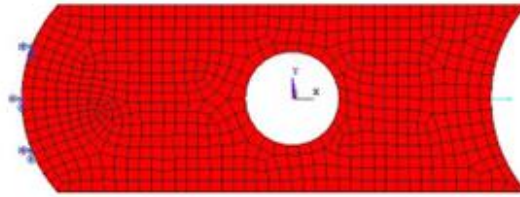


**Figure 3c.** 60 mm Curved Radius

**Figure 3.** Curved Plate

### 3. Analytical Method

The primary purpose of this chapter is to evaluate the accuracy of the finite element model. The maximum stresses for flat plates can be calculated by calculating each hole's stress concentration factor ( $K_t$ ). The model diameter and width values shown in **Figure 4** below can be used to determine the flat plate with hole value of  $K_t$ . The maximum stresses are computed after the  $K_t$  value has been obtained.

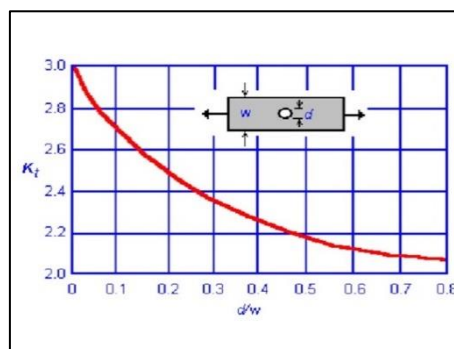


**Figure 4.** Stress Concentration Factor ( $K_t$ ) vs Diameter/Width ( $d/w$ ) Graph for flat plate (Goud & Wani, 2015)

For flat plate:

The maximum stress around the edge of a hole:

$$\sigma_{\max} = K_t \times \sigma_{\text{net}} \quad (1)$$

Where  $\sigma_{\max}$  is the maximum stress in MPa,  $K_t$  is the stress concentration factor and  $\sigma_{\text{net}}$  is the nett stress in MPa

$$\sigma_{\text{net}} = \frac{F}{(w-d)t} \quad (2)$$

Where  $F$  = force in Newton,  $w$  = width of plate in mm,  $d$  = diameter of hole in mm and  $t$  = thickness of the plate in mm

$$\text{Note: } F = 2.5 \text{ N/mm}^2 \times A \quad (3)$$

$$\text{For flat plate: } A = t \times w \quad (4)$$

$$\text{For curve plate: } A = t \times s \quad (5)$$

Where  $A$  = area in  $\text{mm}^2$

$t$  = thickness of plate in mm

$s$  = curve length in mm

**Figure 5, Figure 6** and **Figure 7** describe the calculation for the width ( $w$  and  $s$ ) for both the flat and curve plate.

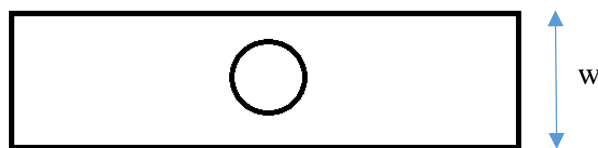


**Figure 5.** Width ( $w$ ) for Flat Plate

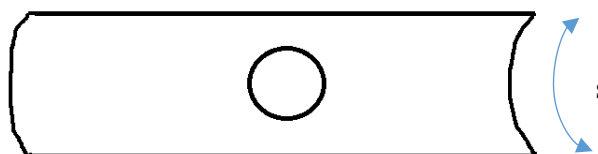


**Figure 6.** Width ( $s$ ) for Curve Plate

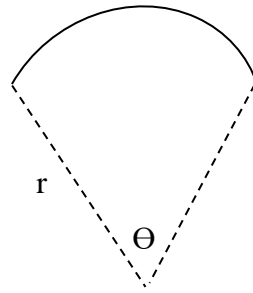


**Figure 7.** Calculation of Width (s) for Curve Plate

Where;  $s = \Theta \times r$  (6)

$\Theta$  in radian

For curve plate:

The stress concentration of the curved plate for each hole can be calculated by the equation below:

$$K_t = \frac{\sigma_{max}}{\sigma_{net}} \quad (7)$$

Where  $K_t$  is the stress concentration factor,  $\sigma_{max}$  is the maximum stress from FE and  $\sigma_{net}$  is the net stress.

## 4. Results and Discussion

The following results were obtained from the finite element analysis. For flat plates, the maximum stresses from finite element analysis are compared to the theoretical stress concentration factor calculation. As there is no stress concentration factor for the curved plate, the maximum stresses from finite element analysis are used to calculate the stress concentration factor for curved plate.

### 4.1 Flat Plate

This section discusses the results from the flat plate analysis.

**Table 3** below describes the stress concentration factor and maximum stress using the analytical method for flat plate. With reducing hole diameter, the maximum stress is decreasing because



of more material is available to carry the load. Stress concentration factor is increasing with decreasing hole diameter.

**Table 3.** Stress Concentration Factor and Maximum Stress using Analytical Method for Flat Plate

Hole Diameter (mm)	Diameter / Width (d/w)	Stress Concentration Factor, $K_t$	Max Stress Using Analytical Method (MPa)
40	0.5	2.19	10.9500
20	0.250	2.40	8.0000
10	0.125	2.62	7.4856

**Figure 8** below shows the relationship between stress concentration factor and d/w. The chart indicates that stress concentration factor increases with decreasing d/w and the relationship is linear.

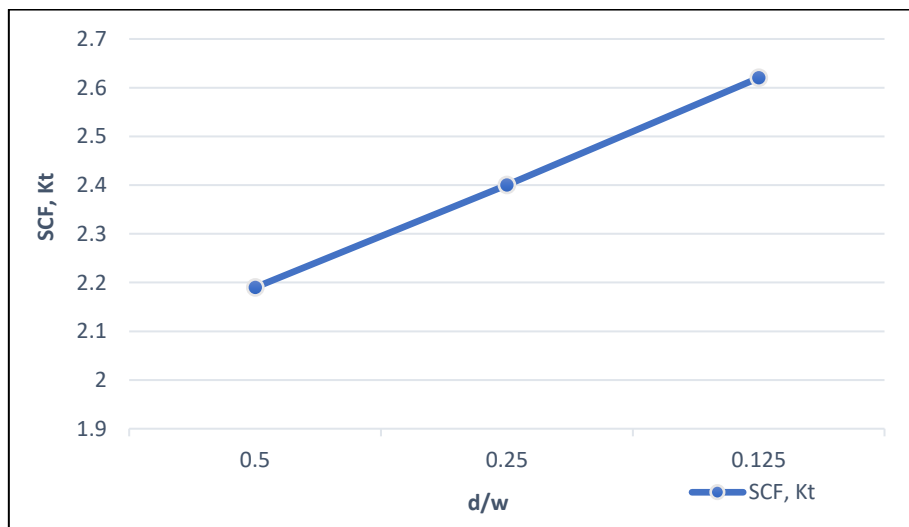


**Figure 8.** Stress Concentration Factor vs (diameter/width) values for Flat Plate

**Figure 9** below demonstrates the flat plate's stress distributions using a 40 mm hole and elements with 5 mm, 4 mm, and 2 mm sizes.

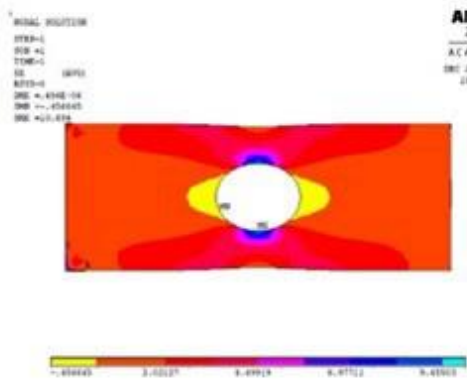


Figure 9a. Stress Distribution (5 mm)

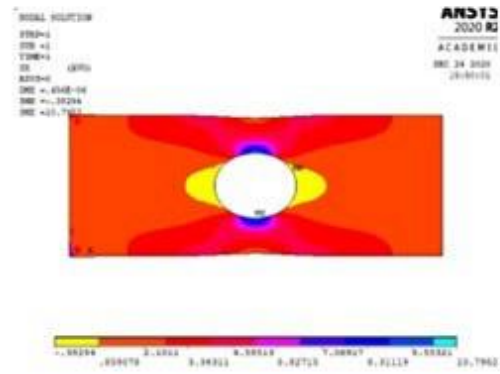


Figure 9b. Stress Distribution (4 mm)

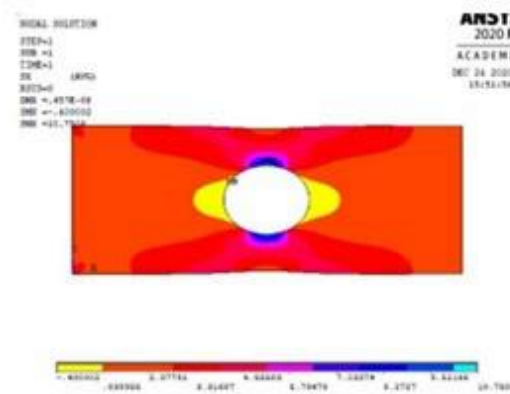


Figure 9c. Stress Distribution (2 mm)

Figure 9. PLA Stress Distribution for Flat Plate

All figures indicate that the maximum stress happens at the edge of the hole and the results obtained for the flat plates are tabulated in **Table 4** below.

**Table 4.** Finite Element Analysis and Analytical Method Comparison of Maximum Stress

Hole Diameter (mm)	Max. Stress Using Analytical Method (MPa)	Max. Stress Using Finite Element Analysis Method (MPa)		
		Element Size		
		5 mm	4 mm	2 mm
40	10.95	10.6940	10.7952	10.7506
20	8.00	7.9051	8.0132	8.04699
10	7.4856	7.3398	7.8728	7.5797

The graph of stresses for flat plate elements with 5 mm, 4 mm, and 2 mm in size vs.  $d/w$  is shown in **Figure 10** below. The chart shows the stress values and compares these stresses calculated by the analytical method and the stresses obtained by the finite element analysis. With smaller hole diameter, as expected the stress is going to be lower due to more material is available to carry the load. The graph demonstrates that the value of stress at a 2 mm element size is practically identical to that calculated using the analytical method. This indicates that a more refined meshing is going to produce more accurate results.

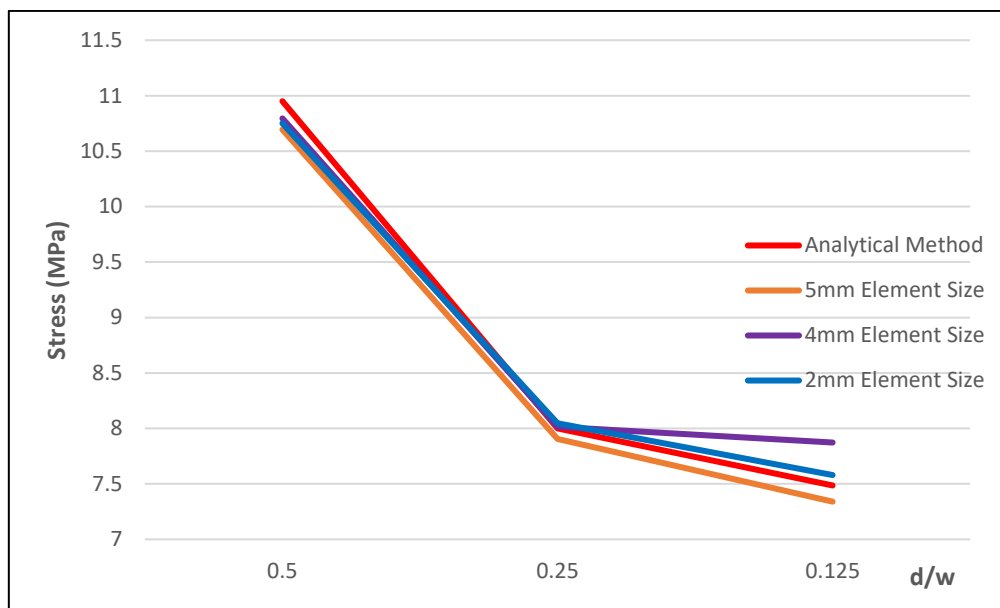


**Figure 10.** Stresses (MPa) vs. (diameter/width) with different element sizes compared to the Analytical Method

#### 4.2 Curve Plate

The stress distribution example for curve radius of 100 mm, 80 mm, and 60 mm with a 40 mm hole is shown in **Figure 11** below. It is also seen that the maximum stress distribution occurs at the edge of the hole.

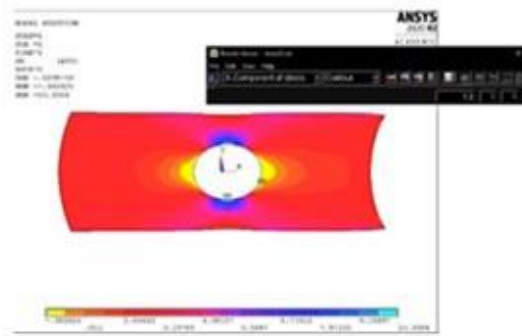


Figure 11a. Radius of 100 mm

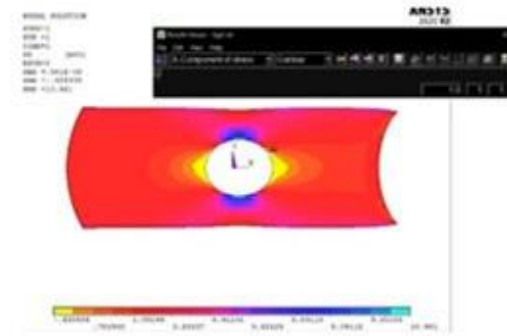


Figure 11b. Radius of 80 mm

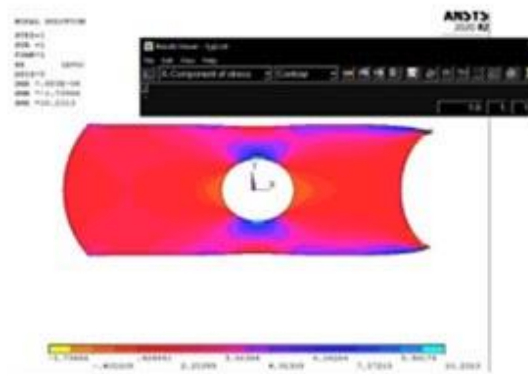


Figure 11c. Radius of 60 mm

Figure 11. Stress Distribution of Curved Plate

Table 5 below displays the maximum stresses derived from finite element analysis for curved plates with 100 mm, 80 mm, and 60 mm curved radius at different hole diameters.

**Table 5.** FEA's Maximum Stress and Stress Concentration Factor

Curve Radius (mm)	Hole Diameter (mm)	Element Size (mm)	Net. Stress (MPa)	Max Stress Using FEA Analysis (MPa)	Stress Concentration Factor (SCF), $K_t$
100	40	5	4.9630	10.3584	2.09
		4		10.9018	2.20
		2		10.7063	2.16
	20	5	3.3170	7.3817	2.23
		4		7.9707	2.40
		2		8.0046	2.41
	10	5	2.8450	7.2117	2.53
		4		7.6880	2.70
		2		7.5529	2.65
80	40	5	4.5660	10.4610	2.29
		4		10.6503	2.33
		2		10.6238	2.33
	20	5	3.1350	7.5125	2.40
		4		7.9342	2.53
		2		8.2088	2.62
	10	5	2.7100	7.1378	2.63
		4		7.5312	2.78
		2		7.4867	2.76
60	40	5	4.1670	10.2313	2.46
		4		10.5643	2.54
		2		10.5938	2.54
	20	5	3.9410	10.1417	2.57
		4		10.3263	2.62
		2		10.2352	2.60
	10	5	2.5640	10.1416	3.96
		4		10.3118	4.02
		2		10.2362	3.99

**Table 5** demonstrate the maximum stress values determined using finite element analysis for curved plates with curves with 100, 80, and 60 mm radiuses various holes diameter. These values show that mesh convergence is dependent on element sizes.

The value of the stress concentration factor can be derived using the maximum stress obtained, as shown in **Table 6**. As shown in **Figure 12**, when the hole diameter of the plate is smaller, the value of  $d/w$  decreases for all the curved plates with varying radiuses. As the radius of the curve decreases, the plate width increases. According to the graph above, the lower the  $d/w$  value, the higher the stress concentration factor. This is because smaller hole diameters are associated with higher stress concentration factors. The lower the maximum stress value produced, the higher the stress concentration factor.

**Table 6.** Highest Stress and Stress Concentration Factor for Curved Plate

Curve Radius (mm)	Hole Diameter, d (m)	Plate Width, w (m)	Diameter / Width	Stress Concentration Factor (SCF), $K_t$
100	0.04	0.0803	0.5	2.18
	0.02		0.25	2.41
	0.01		0.12	2.68
80	0.04	0.0838	0.48	2.33
	0.02		0.24	2.57
	0.01		0.12	2.77
60	0.04	0.0880	0.45	2.54
	0.02		0.23	3.48
	0.01		0.11	3.99

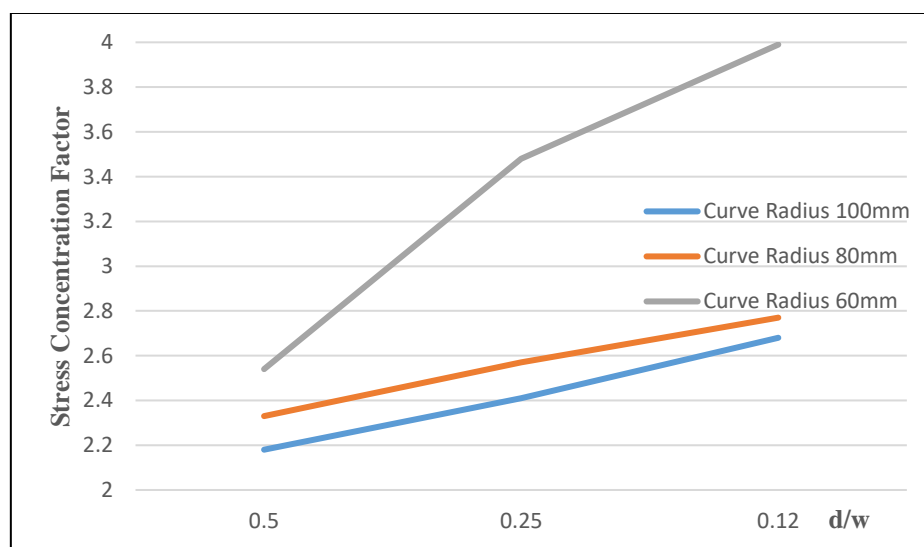


**Figure 12.** Stress Concentration Factor vs. (diameter/width) for 100 mm, 80 mm and 60 mm Curve Radius

### 4.3 Comparison Between Flat and Curve Plate with Holes

In this section, stress concentration factor of the curve plate (**Table 6**) is compared with the flat plate (**Table 3**). If we compare the stress concentration factor of the curve plate with 100 mm curve radius, the stress concentration factor is practically the same for each hole diameter with the flat plate. However, the more curve the plate (reduced curve radius) the stress concentration factor is increasing. This indicates that the flatter the curve plate, the closer the stress concentration factor with the flat plate. Another finding is that the more the curve plate has, the higher the stress concentration. Probably this is due to the induced bending that happens to the curve plate.

## 5. Conclusion

The aim of this study is to investigate the behaviour of flat and curve plate made of PLA in terms of its maximum stress and stress concentration factor. Finite element analysis was used to conduct the investigation. To validate the maximum stresses, the results of finite element analysis of the flat plate were compared to the findings of the analytical technique. For the flat plate, when the element sizes were reduced, the study's results revealed a stress pattern nearly identical to the theoretical result. As expected, the highest stresses were seen next to the hole's edge. The stress concentration factor increases with the decrease of the diameter of the holes in both flat and curved plates. Curve radius is having a significant effect to the stress concentration factor. It can be concluded that understanding the stress pattern is critical in structural design.

## References

- A. Kolodziej, A. B. P. Zur. (2019). Finite Elements Analysis of PLA 3D-printed Elements and Shape Optimization. *European Journal of Engineering Science and Technology*, ISSN2538-9181. <https://doi.org/10.33422/ejest.2019.01.51>
- Agrawal, P., Dhattrak, P., & Choudhary, P. (2021). Comparative study on vibration characteristics of aircraft wings using finite element method. *Materials Today: Proceedings*, 46, 176–183. <https://doi.org/10.1016/j.matpr.2020.07.229>
- Ansell, H. (2015). *A Review of Aeronautical Fatigue Investigations in Sweden During the Period April 2013 to March 2015*. 2431, 1–2.
- Ding, L. Y. . (2006). Simulation of Laser Shock Peening on a Curved Surface (mesh refinement). *Met. Surf. Eng, Woodhead Publications*, 133–150.
- Ertane, E. G., Dorner-Reisel, A., Baran, O., Welzel, T., Matner, V., & Svoboda, S. (2018). Processing and Wear Behaviour of 3D Printed PLA Reinforced with Biogenic Carbon. *Advances in Tribology, 2018*. <https://doi.org/10.1155/2018/1763182>
- Goud, K., & Wani, T. P. (2015). *Stress analysis of the landing gear well beams and damage calculation due to landing cycles*. International Journal of Research in Aeronautical and Mechanical Engineering. [10.13140/RG.2.1.4473.6085](https://doi.org/10.13140/RG.2.1.4473.6085)
- Guduru, K. K., & Srinivasu, G. (2020). Effect of post treatment on tensile properties of carbon reinforced PLA composite by 3D printing. *Materials Today: Proceedings*, 33, 5403–5407. <https://doi.org/10.1016/j.matpr.2020.03.128>
- Jain, N. K., & Mittal, N. D. (2008). Finite element analysis for stress concentration and deflection in isotropic, orthotropic and laminated composite plates with central circular hole under transverse static loading. *Materials Science and Engineering A*, 498(1–2), 115–124. <https://doi.org/10.1016/j.msea.2008.04.078>
- Kim, Y., & Park, J. (2020). A theory for the free vibration of a laminated composite rectangular plate with holes in aerospace applications. *Composite Structures*, 251(May), 112571. <https://doi.org/10.1016/j.compstruct.2020.112571>
- Kuntjoro, W., Roslan, I. S., Muta'ali, A. B. A., Anwar, N. izyan A. K., & Nasir, R. E. M. (2021). A Study of 3D Printed Box Structure. *Journal of Aeronautics, Astronautics and Aviation*, 53(2), 137–142. [https://doi.org/10.6125/JoAAA.202106\\_53\(2\).05](https://doi.org/10.6125/JoAAA.202106_53(2).05)



- Lalehpour, A., & Barari, A. (2016). Post processing for Fused Deposition Modeling Parts with Acetone Vapour Bath. *IFAC-PapersOnLine*, 49(31), 42–48. <https://doi.org/10.1016/j.ifacol.2016.12.159>
- Mekalke, G. C., Kavade, M. V., & Deshpande, S. S. (2009). Analysis of a Plate With a Circular Hole By Fem. *IOSR Journal of Mechanical and Civil Engineering*, 25–30.
- Mo, J. P. T., Cheung, S. C. P., & Das, R. (2019). Thin Plate Deflection. *Demystifying Numerical Models*, 235–255. <https://doi.org/10.1016/b978-0-08-100975-8.00011-4>
- Ngo, T. D., Kashani, A., Imbalzano, G., Nguyen, K. T. Q., & Hui, D. (2018). Additive manufacturing (3D printing): A review of materials, methods, applications and challenges. *Composites Part B: Engineering*, 143(December 2017), 172–196. <https://doi.org/10.1016/j.compositesb.2018.02.012>
- Pawar, P., Ballav, R. A. J., & Kumar, A. (2016). *Finite Element Method Analysis of Rectangular Plate With Circular Hole Using Ansys*. 14(4), 2787–2798.
- Pukale, B., & Amarnadha Reddy, M. (2014). Stress Analysis and Damage tolerance evaluation for wing structure with a large cutout in the bottom skin. *International Journal of Engineering Technology and Sciences*, 2(1), 33–38.
- Raj, S. A., Muthukumaran, E., & Jayakrishna, K. (2018). A Case Study of 3D Printed PLA and Its Mechanical Properties. *Materials Today: Proceedings*, 5(5), 11219–11226. <https://doi.org/10.1016/j.matpr.2018.01.146>
- Thompson, M. ., & Thompson, J. . (2017). ANSYS Mechanical APDL for Finite Element Analysis. In *Elsevier Science*.
- Zappino, E., Filippi, M., Pagani, A., Petiti, M., & Carrera, E. (2020). Experimental and numerical analysis of 3D printed open-hole plates reinforced with carbon fibers. *Composites Part C: Open Access*, 2(May), 100007. <https://doi.org/10.1016/j.jcomc.2020.100007>